NJC Letter

Nanocrystallised titania and zirconia mesoporous thin films exhibiting enhanced thermal stability

Eduardo L. Crepaldi, Galo J. de A. A. Soler-Illia, David Grosso and Clément Sanchez*

Laboratoire de Chimie de la Matière Condensée, Université Pierre et Marie Curie (Paris VI) - CNRS, 4, place Jussieu (T54-E5), 75252, Paris cedex 05, France. E-mail: clems@ccr.jussieu.fr; Fax: +33 1 44 27 47 69; Tel: +33 1 44 27 33 65

Received (in Montpellier, France) 4th June 2002, Accepted 9th September 2002
First published as an Advance Article on the web 18th October 2002

Tuned chemical conditions complemented with a set of treatments have been developed to enhance the thermal stability of transition metal oxide mesoporous thin films (up to 500 °C for TiO_2 and 450 °C for ZrO_2), allowing the formation of crack-free coatings presenting excellent optical quality (transmittance higher than 85% in the visible region), tailored thickness (from 50 to 700 nm), a highly organised cubic (*Im3m* space group for TiO_2) or 2D-hexagonal (*P6m* space group for ZrO_2) mesostructure, high surface area (140–200 $m^2\ g^{-1}$), controlled and narrowly distributed mesopore size (25–80 Å), and a nanocrystalline inorganic framework (anatase or tetragonal zirconia).

The field of mesoporous materials has experienced a burst of activity in the last decade following the supramolecular template approach introduced by scientists at Mobil Research and Development Co.[1] In this field most of the research has been devoted to silica-based materials,[1,2] which are very versatile in terms of functionalisation with organic groups[3] and stable under thermal treatment. Indeed, the resulting periodically organised mesoporous and amorphous silica frameworks easily keep their integrity upon calcination at temperatures of about 600 °C. The synthesis of transition metal (TM) oxide based mesoporous materials is more difficult than that of silica-based ones, in view of the complexity of TM chemistry, such as high reactivity towards hydrolysis/condensation, and their variable oxidation states and co-ordination numbers. In addition, metal-oxo polymers tend to form crystalline phases upon thermal treatment, whose formation is usually associated with the collapse of the mesoporous network.[4–6]

Among the developed methods, the so-called evaporation-induced self-assembly (EISA)[7,8] is one that has been proven to be especially well-adapted to the design of TM oxide based mesoporous materials.[9–12] In our approach, metal chlorides in alcoholic water media are used as the inorganic source and non-ionic poly(ethylene oxide) based surfactants or block copolymers as the structure-directing agents.[11–14] More recently, other methods based on the use of titania nanoparticles[15] or $Ti(OEt)_4$[16,17] as inorganic precursors and non-ionic poly(ethylene oxide) based surfactants have been developed for the formation of mesoporous TiO_2 based thin films. These authors claimed that the mesostructured coatings are stable up to 400–450 °C, but no evidence for the presence of crystalline anatase phases was presented in these works. Especially for TiO_2, many potential applications (such as photocatalysis and energy conversion) are directly dependent on the presence of anatase. For ZrO_2, even though not essential for the expected potential applications (based on the high stability of this oxide, such as heavy-duty membranes), the crystallisation of the inorganic framework can enhance chemical and/or mechanical stability.

In the present work we report for the first time, to the best of our knowledge, the reproducible synthesis of thermally stable transition metal oxide thin films presenting a periodically organised mesoporosity with high surface area associated with nanocrystalline inorganic walls and an excellent optical quality. The strategies employed to reduce the contraction of the mesostructure and enhance the thermal stability are based on the controlled ageing of the films at increasing temperatures to gradually eliminate volatile species and to further tune the condensation steps, consolidating the inorganic framework before the elimination of the template. Such coatings present a pre-stiffened inorganic network that can be slowly heated up to temperatures of 450 °C for TiO_2 and 400 °C for ZrO_2 to result in highly organised nanocrystalline transition metal oxide mesoporous films.

$TiCl_4$ or $ZrCl_4$ was first reacted with a solution of the template in anhydrous ethanol (ethanol was chosen as solvent due to its substrate wetting properties and the good solubility of all inorganic and organic precursors) to form, as previously described, metallic chloroethoxide precursors [$MCl_{4-x}(OEt)_x$; M = Ti, Zr].[18,19] To this highly acidic system (on average two moles of HCl are generated for each mole of metal chloride), water was added in controlled quantities. From these sols, the deposition process was conducted in controlled atmospheric relative humidity (RH), a parameter of paramount importance for combining good optical quality and high structural order in the resulting coatings.

In-situ SAXS coupled to interferometry analysis showed[20–23] that the formation of meso-organised coatings takes place through a disorder-to-order transition, from an isotropic sol or gel to a worm-like mesophase, to a highly organised cubic *Im3m* [for TiO_2, Fig. 1(a)][24] or 2D-hexagonal *P6m* [for ZrO_2, Fig. 1(b)] mesostructure. For TiO_2, to allow such a transition, two main conditions must be respected: (1) the condensation of the inorganic framework should be quenched and (2) the solvent evaporation (especially water) should be slow. Both conditions contribute to reduction of the viscosity of the deposited gel and allow the formation of micelles, their organisation in a "titanotropic" hybrid liquid crystal mesophase,[10] and their alignment along the film–substrate and film–air interfaces. These conditions can be obtained by using very acidic initial solutions (the applied dipping sols display pH < 0) and carrying out the deposition process at high (≥50%) RH.[20,21]

Indeed, at low temperature (25–35 °C) and in such highly acidic conditions (pH < 0) the ability of titanium(IV) precursors to undergo condensation reactions is strongly quenched and therefore mainly monomeric or small oligomeric titanium

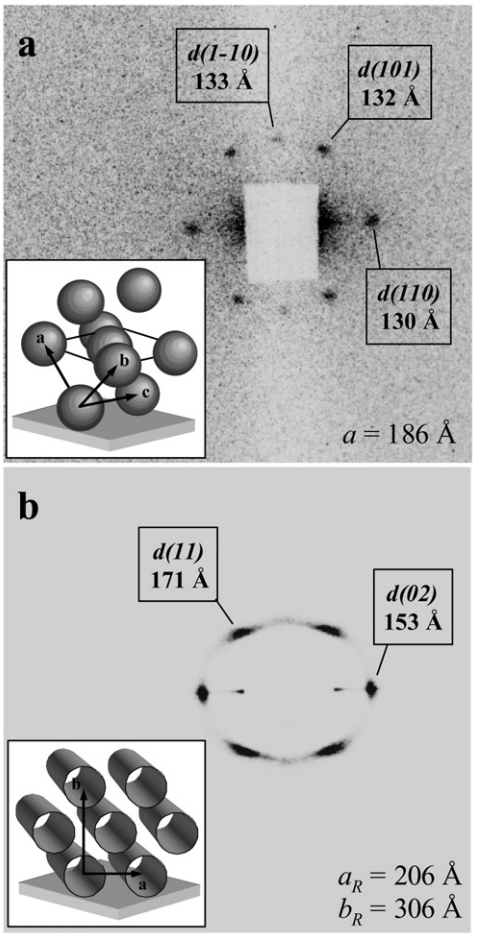

Fig. 1 2D-SAXS patterns for as-prepared F127-templated (a) TiO_2 and (b) ZrO_2 based hybrid mesostructured thin films. The insets in parts (a) and (b) are representations of the cubic (*Im3m*) and hexagonal (*P6m*) unit cells, respectively. The latter is indexed following the *C2m* space group symmetry.

hydroxy species are formed.[25] These species are small, hydrophilic (hydroxylated and hydrated) and may be positively charged when larger amounts of water are present in the solution;[26] these advantages allow a good matching of the hybrid organic-inorganic interface, therefore facilitating co-operative self-assembly processes with the surfactant.[10]

Once the cubic hybrid mesophase has been formed a series of chemical and thermal treatments have been developed to enhance the thermal stability of TiO_2 mesoporous thin films, allowing the formation of highly organised, high surface area mesoporous coatings, exhibiting semicrystalline frameworks. Since the as-prepared film is almost uncondensed, it presents a relatively fragile mesostructure (as-prepared films can be dissolved in water and they contain a large amount of volatile species (15–20 mass % eliminated up to 100 °C, as observed by TG/DSC analysis) and chloride (0.3 to 1 Cl/Ti molar ratio, as observed by EDX)). As a consequence, the method chosen to eliminate the volatile species, to increase the condensation of the inorganic moieties and eliminate the template, is of paramount importance because it determines the integrity of the organisation, the degree of contraction and the thermal stability of the final mesoporous coating. Therefore, a set of ageing treatments under controlled relative humidity followed by progressive thermal treatments (from 60 °C to 500 °C) were carried out.

During these steps, while water from controlled air humidity is provided to the hybrid film, HCl molecules are progressively removed (as determined by EDX for different ageing times). These chemical conditions combined with the thermal treatments allow a progressive condensation of the titanium-oxo network. Indeed, the decrease in acidity, the increase of the water concentration, and the rise in temperature (steps at 60 and 130 °C) produce highly favourable conditions to permit further condensation without surfactant removal. Such a pre-treatment, aimed at pre-consolidating the network, is followed by the removal of templates at temperatures higher than 300 °C without destroying the periodically organised mesostructure. Moreover, when large amphiphilic block copolymers are used as the template they provide thicker amorphous metal-oxo walls that can more easily accommodate the crystallisation of titania nano-anatase.

For ZrO_2 based systems, the formation of extended metal-oxo polymers is much more dependent on the concentration than for Ti(IV).[25] As a result, the evaporation process readily results in the formation of condensed inorganic species and a worm-like mesophase is "frozen". However, the freshly formed zirconium-oxo polymers contain many hydroxo bridges (olation is kinetically favoured[27]) and can be "dissolved".[12] Therefore, a treatment at very high humidity (saturated, exposition to water vapours) for a short time (10–15 s) results in a fast swelling of the film, allowing the disorder-to-order transition. The second drying process takes place homogeneously, enhancing the optical quality. This treatment is more efficient if applied as soon as the first drying process is finished (oxolation is thermodynamically favoured[27]), so the deposition should be carried out in a low humidily atmosphere (10%) for fast evaporation.[12] The further steps of ageing and calcination induce in a first approximation the same effects as those described for titania-based films.

The adhesion of the TiO_2 and ZrO_2 based films to the substrate results in an anisotropic contraction,[28] clearly observed by XRD, 2D-XRD, 2D-SAXS and TEM, resulting in a distorted cubic or 2D-hexagonal structure, which can be respectively described as triclinic or 2D-centred rectangular [space group *C2m*, see inset in Fig. 1(b)].[11,12,18] Results acquired by XRD in $\theta - 2\theta$ mode (Fig. 2) show the importance of ageing and gradually heating the films before calcination at temperatures high enough to eliminate the template. A 1 day old (at room temperature and RH = 50%) F127-templated TiO_2 film (Conditions 1) treated at 350 °C undergoes a structural contraction of about 70% (d_{110}, from approximately 130 to 39 Å). On the other hand, a 2 week old film (at room temperature and RH = 50%), heated at 60 °C for 24 hours followed by 130 °C for 24 hours (Conditions 2), and finally calcined at 350 °C displays a much smaller structural contraction, around 57%. Similar results are observed for both templates (Brij 58 and Pluronic F127) and also for ZrO_2 based systems. A lower degree of contraction means that the resulting coatings can have larger and less distorted pores. In addition, an

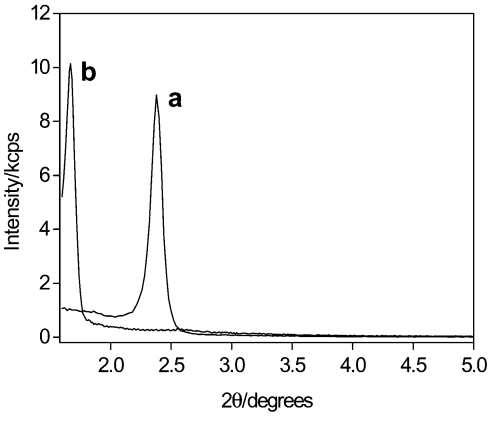

Fig. 2 X-Ray diffraction diagrams for 350 °C treated F127-templated TiO_2 films previously aged following (a) conditions 1 and (b) conditions 2.

enhancement in the thermal stability has been observed, with films treated under conditions 2 undergoing mesostructural collapse in temperatures about 50 to 100 °C higher than those treated under conditions 1, which is crucial for the formation of highly organised, high surface area semicrystalline coatings (see below).

Fig. 3 summarises the results obtained for the thermal treatment of Pluronic F127-templated TiO_2 based mesostructured films. Low-angle XRD in $\theta - 2\theta$ mode [Fig. 3(a)] shows a gradual reduction of d_{110} and a decrease in the peak intensity for treatment between 350 and 450 °C. The intense and narrow peaks (FWHM $\approx 0.1°$) suggest a very highly organised and oriented mesostructure, which can be seen by TEM [Fig. 3(c)]. At 500 °C a marked reduction in intensity and broadening of the [110] peak (FWHM $\approx 0.4°$) suggests a degradation of the structure, with further heating resulting in mesostructural collapse. Wide-angle XRD in parallel mode clearly shows the formation of anatase from 400 °C [Fig. 3(b)]. At 450 and 500 °C, besides the presence of anatase, low intensity peaks arising from the presence of brookite (JCPDS, PDF card no. 29–1360) can be observed. Finally, heating at 600 °C results in coatings presenting only anatase, showing that the brookite phase is metastable. HRTEM [Fig. 3(e)] analysis showed the presence of an important quantity of anatase crystallites for films treated at 350 °C and above. The problem to detect such a phase by XRD for the 350 °C treated film is strictly related to the small quantity of matter in the coatings associated with the small size of the crystallites (broad peaks). Thick films (4 layers) were prepared by a dip-coating/stabilisation at 130 °C/dip-coating process to increase the deposited quantity of matter. Analysing the resulting film treated at 350 °C (following conditions 2) by XRD showed the presence of an intense peak at *ca.* 1.73° (2θ), very close to that observed for a similar monolayer film. The peak is slightly broader (FWHM $\approx 0.2°$), which indicates a lower order and/or lower orientation of the mesophase. In such a film, the deposited quantity of matter is enough to detect the crystalline phase (anatase) by XRD, as one can see in Fig. 3(d).

As revealed by TEM and HRTEM [Figs. 3(c) and 3(e)], the thickness of the pore walls of films treated at and above 300 °C is approximately 100 Å (dark areas). From the results presented in Figs. 3(a) and 3(b) one can see that the degradation of the structure can be directly related to the formation of anatase crystallites [see inset in Fig. 3(b)] that exceed this size, which occurs from 450 to 500 °C. Therefore, highly organised mesoporous TiO_2 thin films exhibiting a semicrystalline (anatase) framework can be obtained by thermally treating aged films at temperatures ranging from 350 and 450 °C. Under such conditions, the 300–400 nm thick (as determined by ellipsometry[11] and checked by TEM and SEM) coatings present excellent optical quality (transmittance > 85% from 350 to 1100 nm), high surface area (148 $m^2\ g^{-1}$ for a 350 °C treated film, see Fig. 4) and are totally crack-free on the micrometric scale (as observed by SEM). The pore size of the resulting coatings is large, around 58 Å, and narrowly distributed (FWHM ≈ 25 Å), in good agreement with the elliptical (approximately 40×80 Å) pores observed by TEM. As one

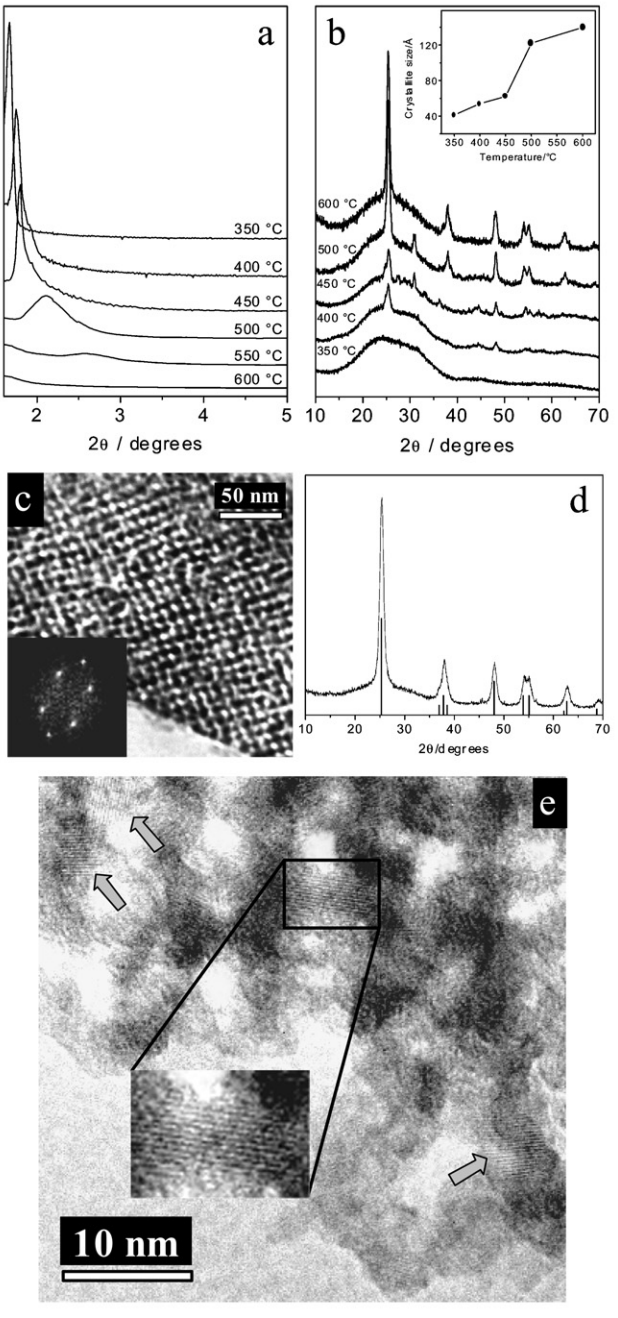

Fig. 3 F127-templated TiO_2 films prepared following conditions 2: (a) low-angle ($\theta - 2\theta$ mode) and (b) wide-angle (parallel mode) XRD diagrams for films treated at the indicated temperatures. The inset in part (b) shows the variation of the anatase crystallite size as a function of temperature. (c) TEM image along the [111] zone axis for a 350 °C treated film. The inset in part (c) is the modulus of the Fourier transform of the full image. (d) Wide-angle XRD pattern for a multilayer (4 coatings) 350 °C treated film together with the lines for anatase (JCPDS, PDF card no. 21-1272), from which the crystallite size for the 350 °C treated sample was calculated. (e) HRTEM images along the [100] zone axis for a 400 °C treated film showing the presence of anatase crystallites.

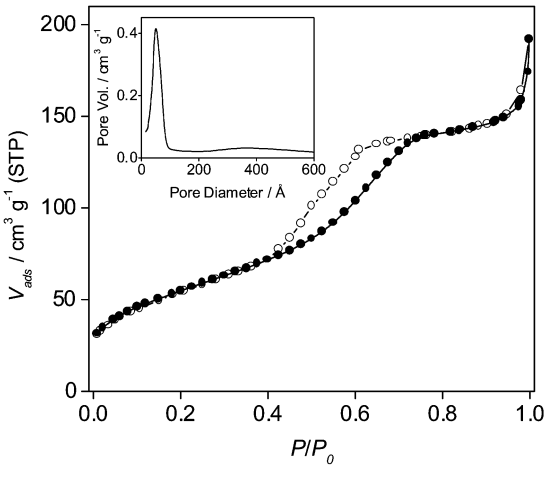

Fig. 4 Nitrogen adsorption-desorption isotherms and pore size distribution plot for 350 °C treated a F127-templated TiO_2 film.

can see in Fig. 4, the volume adsorbed at low pressure is not large, showing that the surface area comes practically only from the mesopores, unlike PEO based block copolymer templated silicas.[29] In this type IV isotherm it is difficult to identify the hysteresis loop as H1 or H2.[30] Usually, the N_2 adsorption isotherms of materials presenting a cage-like structure (such as the mesostructure observed here for F127-templated TiO_2 films, *Im*3*m* symmetry) have a H2 hysteresis loop, associated with the presence of large pores connected by smaller openings (ink-bottle pores), typical of SBA-16[29] and also observed for F127-templated silica films.[31] Here, this effect seems to be minimised by the presence of defects in the pore walls, as one can see in Fig. 3(c).

ZrO_2 based mesostructured films treated up to 300 °C present very high structural order [Figs. 5(a) and 5(c)]. Treatment at 350 and 400 °C results in a gradual reduction in intensity and broadening of the (02) XRD peak, as well as a progressive structural contraction. A very broad, low intensity peak can be observed at 450 °C, while at 500 °C the mesostructure is completely lost. Wide-angle XRD showed very broad, low intensity peaks [indicated by arrows in Fig. 5(b)] for films treated between 300 and 400 °C. The broadness (FWHM $> 2°$) of such peaks indicates that crystallites smaller than 40 Å are present in the ZrO_2 framework, which can be easily detected by HRTEM [Fig. 5(d)]. Further heating (to 450 and 500 °C) results in a massive crystallisation of the inorganic network, and the resulting wide-angle XRD patterns display intense peaks that show the presence of tetragonal zirconia (JCPDS, PDF card no. 50-1089). The size of the crystallites quickly grows from less than 40 Å (at 400 °C) to more than 100 Å (at 450–500 °C), exceeding the thickness of the pore walls (around 80 Å, as estimated by TEM), which results in mesostructural collapse. However, the coatings treated between 300 and 400 °C exhibit excellent optical quality (films are crack-free and transparent, with transmittance higher than 90% in the 200 to 1100 nm region for a typical thickness of 300 nm), high structural order and a semicrystalline (tetragonal zirconia) framework.

When Brij 58 (B58) was used as the structure-directing agent a much lower thermal stability was attained for both ZrO_2 and TiO_2 based systems. TiO_2 based coatings maintain their mesostructural stability up to 350 °C,[11] while the stability of ZrO_2 based ones is limited to 300 °C.[12] The B58-templated coatings have similar porosity (estimated based on the organic/inorganic ratio) to those templated by F127, however, the size of the micelles of B58 are much smaller, resulting in much smaller pores and thinner walls (around 25 Å for both TiO_2 and ZrO_2 based thin films). These thin walls cannot accommodate the crystallites formed at temperatures higher than those indicated above. These results support the hypothesis that the mesostructural degradation can be related to indiscriminate crystallisation of the inorganic framework, with crystallites growing to a size that exceeds the thickness of the pore walls. Nevertheless, anatase nanocrystallites could be observed in the inorganic walls of 350 °C treated B58-templated TiO_2 films by HRTEM.[20–23]

Moreover, preliminary results indicate that following the same synthesis strategy the preparation of mixed oxide (such as ZrO_2–CeO_2) mesoporous films is feasible and results in higher thermally stable mesoporous coatings, in which the high structural order can be retained up to 500 °C.

The results presented in this letter open a wealth of opportunities to synthesise non-silicate nanocrystalline mesoporous coatings with relevance for use as materials in the field of catalysis, photocatalysis and nano-membranes working under extreme conditions (for instance high pH and temperature).

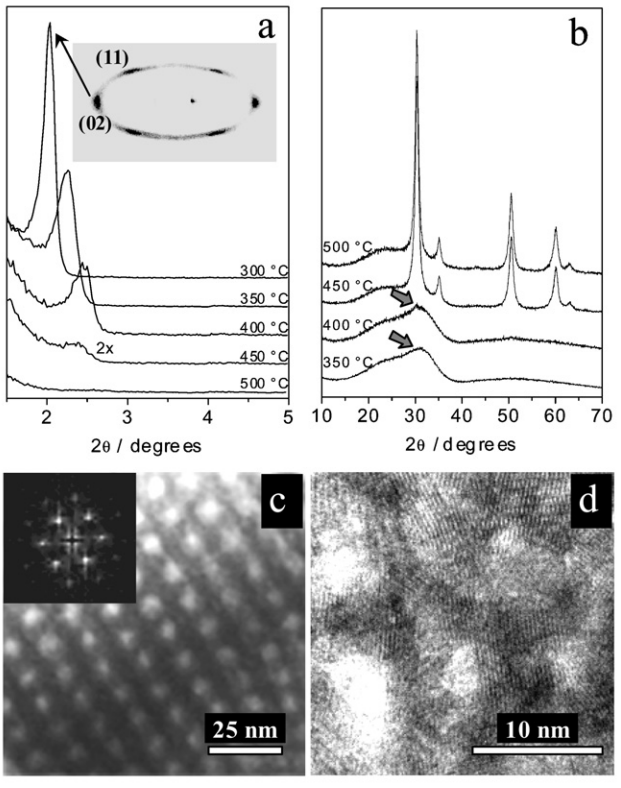

Fig. 5 F127-templated ZrO_2 films prepared following conditions 2: (a) low-angle ($\theta - 2\theta$ mode) and (b) wide-angle (parallel mode) XRD diagrams for films treated at the indicated temperatures. The inset in part (a) is a 2D-SAXS pattern for a 300 °C treated film. (c) TEM and (d) HRTEM images along the [001] zone axis for a 300 °C treated film. The inset in part (c) is the modulus of the Fourier transform of the full image.

Experimental

Film preparation

The starting solutions contain 1 $TiCl_4$:*t* template:40 EtOH:10 H_2O or 1 $ZrCl_4$:*t* template:40 EtOH:20 H_2O, where *t* is 0.05 for Brij 58 [$C_{16}H_{33}(OCH_2CH_2)_{20}OH$] or 0.005 for Pluronic F-127 [$HO(CH_2CH_2O)_{106}(CH_2CH(CH_3)O)_{70}(CH_2CH_2O)_{106}H$]. In both cases, *t* was adjusted in order to give approximately one ethylene oxide (EO) group per metal, resulting in an inorganic (MO_2)/organic ratio around 0.3–0.4 (v/v). The preparation of a typical dipping solution can be described as follows: 0.01 mol of anhydrous metal chloride (1.93 g for $TiCl_4$ or 2.33 g for $ZrCl_4$) was slowly added to a solution containing 0.57 g of Brij 58 or 0.67 g of Pluronic F-127 in 18.43 g of ethanol. To this solution 1.80 g (for Ti) or 3.60 g (for Zr) of water was slowly added.

Films were prepared by dip-coating glass or silicon substrates at a constant withdrawal rate (1–5 mm s^{-1}) at controlled temperature (25–35 °C) and relative humidity (RH, 10–80%). After a given ageing time at controlled RH, the films were thermally treated in air (ramp of 1 °C min^{-1}) at temperatures ranging from 60 to 600 °C.

Film characterisation

Low-angle X-ray diffraction (XRD) diagrams were collected in $\theta - 2\theta$ mode using a conventional goniometer, PW 1820 Philips (Cu-Kα_1 radiation, $\lambda = 1.5406$ Å). Wide-angle XRD patterns were collected in parallel mode ($\omega = 0.5°$, 2θ varied from 10 to 70°, Cu-Kα_1 radiation) using a Philips X'Pert PW-3050 with a thin film optic. The crystallite size was estimated by applying the Scherrer equation to the FWHM of the (101) peak for anatase and tetragonal zirconia, with silicon as a standard for the instrumental line broadening. Synchrotron

small-angle X-ray scattering (SAXS) analysis was performed in transmission mode using the synchrotron radiation of the SAXS beam-line of ELETTRA (Trieste, Italy). Full details regarding such experiments can be found elsewhere.[13,14,20,21,32,33]

Transmission electron microscopy images in ordinary (TEM) or high (HRTEM) resolution were collected using a Philips EM 208 (120 kV) or a Philips CM 20 (200 kV) microscope, respectively, for samples scratched from the substrate, embedded in epoxy resin, and ultramicrotomised. Scanning electron microscopy coupled to EDX investigations (JEOL JSM-5200 scanning microscope operating at 20 kV, coupled to an Oxford Link Pentafet 6880 for surface elemental analysis) were performed to evaluate the morphology and the chemical composition of the film surface.

Ultraviolet-visible spectrophotometry was performed using a Bio-Tek Instruments UVIKON XS spectrophotometer for films deposited on fused silica substrates.

Thermogravimetric (TGA)/differential scanning calorimetric (DSC) analysis was performed in air (100 cm^3 min^{-1}) using a TA Instruments SDT 2960 from room temperature to 700 °C at a heating rate of 1 °C min^{-1}. Nitrogen adsorption-desorption isotherms were collected at −196 °C for films scratched from the substrate using Micromeritics ASAP 2010 equipment (BET and BJH models, respectively, used for surface area and porosity evaluation).

Acknowledgements

This work was financially supported by the French Ministry of Research, CNRS, CNPq (Brazil, grant no. 200636/00-0), and Fundación Antorchas (Argentina). The authors thank Dr. Pierre-Antoine Albouy and Dr. Heinz Amenitsch for their help with the Synchrotron-SAXS measurements. The authors also thank José A. Maulin and Maria T. P. Maglia, and the Laboratório de Microscopia Eletrônica of the Depto. de Biologia Celular Molecular e Bioagentes Patogênicos, Faculdade de Medicina de Ribeirão Preto, University of São Paulo, for TEM measurements.

References

1 (*a*) C. T. Kresge, M. E. Leonowicz, W. J. Roth, J. C. Vartuli and J. S. Beck, *Nature*, 1992, **359**, 710; (*b*) J. S. Beck, J. C. Vartuli, W. J. Roth, M. E. Leonowicz, C. T. Kresge, K. D. Schmitt, C. T.-W. Chu, D. H. Olson, E. W. Sheppard, S. B. McCullen, J. B. Higgins and J. L. Schlenker, *J. Am. Chem. Soc.*, 1992, **114**, 10 834.

2 (*a*) A. Corma, *Chem. Rev.*, 1997, **97**, 2373; (*b*) J. Y. Ying, C. Mehnert and M. S. Wong, *Angew. Chem., Int. Ed.*, 1999, **38**, 57; (*c*) T. J. Barton, L. M. Bull, W. G. Klemperer, D. A. Loy, B. McEnaney, M. Misono, P. A. Monson, G. Pez, G. W. Scherer, J. C. Vartuli and O. M. Yaghi, *Chem. Mater.*, 1999, **11**, 2633; (*d*) D. Zhao, P. Yang, Q. Huo, B. F. Chmelka and G. D. Stucky, *Curr. Opin. Solid State Mater. Sci.*, 1998, **3**, 111; (*e*) N. K. Raman, M. T. Anderson and C. J. Brinker, *Chem. Mater.*, 1996, **8**, 1682.

3 (*a*) A. Stein, B. J. Melde and R. C. Schroden, *Adv. Mater.*, 2000, **12**, 1403; (*b*) A. Sayari and S. Hamoudi, *Chem. Mater.*, 2001, **13**, 3151.

4 A. Sayari and P. Liu, *Microporous Mater.*, 1997, **12**, 149.

5 F. Schüth, *Chem. Mater.*, 2001, **13**, 3184.

6 G. J. de A. A. Soler-Illia, C. Sanchez, B. Lebeau and J. Patarin, *Chem. Rev.*, 2002, **102**(11), in press.

7 Y. Lu, R. Ganguli, C. A. Drewien, M. T. Anderson, C. J. Brinker, W. Gong, Y. Guo, H. Soyez, B. Dunn, M. H. Huang and J. I. Zink, *Nature*, 1997, **389**, 364.

8 C. J. Brinker, Y. Lu, A. Sellinger and H. Fan, *Adv. Mater.*, 1999, **11**, 579.

9 (*a*) P. Yang, D. Zhao, D. I. Margolese, B. F. Chmelka and G. D. Stucky, *Nature*, 1998, **395**, 583; (*b*) P. Yang, D. Zhao, D. I. Margolese, B. F. Chmelka and G. D. Stucky, *Chem. Mater.*, 1999, **11**, 2813.

10 (*a*) G. J. de A. A. Soler-Illia, E. Scolan, A. Louis, P. A. Albouy and C. Sanchez, *New J. Chem.*, 2001, **25**, 156; (*b*) G. J. de A. A. Soler-Illia, A. Louis and C. Sanchez, *Chem. Mater.*, 2002, **14**, 750; (*c*) G. J. de A. A. Soler-Illia and C. Sanchez, *New J. Chem.*, 2000, **24**, 493.

11 D. Grosso, G. J. de A. A. Soler-Illia, F. Babonneau, C. Sanchez, P.-A. Albouy, A. Brunet-Bruneau and A. R. Balkenende, *Adv. Mater.*, 2001, **13**, 1085.

12 E. L. Crepaldi, G. J. de A. A. Soler-Illia, D. Grosso, P.-A. Albouy and C. Sanchez, *Chem. Commun.*, 2001, 1582.

13 L. Pidol, D. Grosso, G. J. de A. A. Soler-Illia, E. L. Crepaldi, C. Sanchez, P.-A. Albouy, H. Amenitsch and P. Euzen, *J. Mater. Chem.*, 2002, **12**, 557.

14 E. L. Crepaldi, D. Grosso, G. J. de A. A. Soler-Illia, P.-A. Albouy, H. Amenitsch and Clément Sanchez, *Chem. Mater.*, 2002, **14**, 3316.

15 Y. K. Hwang, K.-C. Lee and Y.-U. Kwon, *Chem. Commun.*, 2001, 1738.

16 H. Yun, K. Miyazawa, H. Zhou, I. Honma and M. Kuwabara, *Adv. Mater.*, 2001, **13**, 1377.

17 K. L. Frindell, M. H. Bartl, A. Popitsch and G. D. Stucky, *Angew. Chem., Int. Ed.*, 2002, **41**, 960.

18 D. C. Bradley, R. C. Mehrotra and D. P. Gaur, *Metal Alkoxides*, Academic Press, London, 1978.

19 M. Nabavi, S. Doeuff, C. Sanchez and J. Livage, *J. Non-Cryst. Solids*, 1990, **121**, 31.

20 E. L. Crepaldi, G. J. de A. A. Soler-Illia, D. Grosso, P.-A. Albouy, H. Amenitsch and C. Sanchez, *Stud. Surf. Sci. Catal.*, 2002, **141**, 235.

21 D. Grosso, F. Babonneau, C. Sanchez, G. J. de A. A. Soler-Illia, E. L. Crepaldi, P.-A. Albouy, H. Amenitsch, A. R. Balkenende and A. Brunet-Bruneau, *J. Sol-Gel Sci. Technol.*, 2003, in press.

22 C. Sanchez, E. L. Crepaldi, A. Bouchara, F. Cagnol, D. Grosso and G. J. de A. A. Soler-Illia, *Mater. Res. Soc. Symp. Proc.*, 2002, **728**, S1-2.

23 G. J. de A. A. Soler-Illia, D. Grosso, E. L. Crepaldi, F. Cagnol and C. Sanchez, *Mater. Res. Soc. Symp. Proc.*, 2002, **726**, Q7.3.

24 According to the angles between the in-plane and out-of-plane spots in the 2D-SAXS pattern, the cubic domains are oriented with the (110) plane (the most densely packed in the lattice) parallel to the substrate. A complete indexation of a similar mesophase presenting the same orientation was reported for F127-templated silica thick films in: G. J. de A. A. Soler-Illia, E. L. Crepaldi, D. Grosso, D. Durand and C. Sanchez, *Chem. Commun.*, 2002, 2298.

25 C. F. Baes and R. E. Mesmer, *The Hydrolysis of Cations*, John Wiley & Sons, New York, 1976.

26 M. G. Reichmann, F. J. Hollander and A. T. Bell, *Acta Crystallogr., Sect. C*, 1987, **43**, 1681.

27 E. M. Larsen, in *Advances in Inorganic Chemistry and Radiochemistry*, eds. H. J. Emeléus and A. G. Sharpe, Academic Press, New York, 1970, vol. 13, p. 1.

28 M. Klotz, P.-A. Albouy, A. Ayral, C. Ménager, D. Grosso, A. Van der Lee, V. Cabuil, F. Babonneau and C. Guizard, *Chem. Mater.*, 2000, **12**, 1721.

29 D. Zhao, Q. Huo, J. Feng, B. F. Chmelka and G. D. Stucky, *J. Am. Chem. Soc.*, 1998, **120**, 6024.

30 M. Kruk and M. Jaroniec, *Chem. Mater.*, 2001, **13**, 3169.

31 D. Zhao, P. Yang, N. Melosh, J. Feng, B. F. Chmelka and G. D. Stucky, *Adv. Mater.*, 1998, **10**, 1380.

32 D. Grosso, A. R. Balkenende, P.-A. Albouy, A. Ayral, H. Amenitsch and F. Babonneau, *Chem. Mater.*, 2001, **13**, 1848.

33 D. Grosso, F. Babonneau, P.-A. Albouy, H. Amenitsch, A. R. Balkenende, A. Brunet-Bruneau and J. Rivory, *Chem. Mater.*, 2002, **14**, 931.